# Measurement of the $L_2$-$L_3$ Coster-Kronig transition probability in Pb ($Z=82$)

A. L. Catz
*University of Massachusetts at Boston, Boston, Massachusetts 02125*
(Received 8 April 1987)

The value of the $L_2$-$L_3$ Coster-Kronig transition probability ($f_{23}$) in Pb has been determined by multiparameter $K$ versus $L$ x-ray coincidence measurements using high-energy-resolution germanium and silicon detectors. The Pb x rays were obtained from a radioactive source of $^{207}$Bi. A new method of data analysis to determine the contribution of $K\alpha_1$ x rays to the $K\alpha_2$ x-ray peak is described. Precise determination of this contribution is crucial to accurate measurement of $f_{23}$. The value obtained, $f_{23}=0.112\pm0.001$, is slightly lower than predicted by the latest theoretical calculations. A trend toward deviations from theory in the same direction appears to be confirmed by recently measured values of $f_{23}$ in other medium- and high-$Z$ atoms.
MS code no. AD3623 1987 PACS number(s): 32.30.Rj, 32.80.Hd

## I. INTRODUCTION

Coster-Kronig transition probabilities in high-$Z$ atoms have been the subject of numerous experimental and theoretical works[1–6] during the last two decades. The $L_2$-$L_3$ Coster-Kronig transition probability $f_{23}$ in particular has been intensely studied[7–13] since it is amenable to precision measurement by $K$ versus $L$ x-ray coincidence techniques thus offering a valuable test point for comparison with theoretical calculations.[4–6,14,15]

The most commonly used method of measuring $f_{23}$ is based on the study of x-ray cascades which start with a vacancy in the $K$ shell. In such studies, radioactive nuclides which involve in their decay, processes of $K$-shell electron capture, or $K$-shell internal conversion, are usually employed as the sources of x rays.

The method[16,17] (see also Refs. 1 and 11) consists of the measurement of the spectra of $L$ x rays in coincidence with $K\alpha_1$ and $K\alpha_2$ x rays and the calculation of $f_{23}$ from the formula

$$f_{23}=\frac{C_{L\alpha}(K\alpha_2)}{C_{L\alpha}(K\alpha_1)}\frac{n(K\alpha_1)}{n(K\alpha_2)}W(\theta)\ . \tag{1}$$

$C_{L\alpha}(K\alpha_2)$ and $C_{L\alpha}(K\alpha_1)$ are the numbers of $L\alpha$ x-ray photons detected in coincidence with $K\alpha_2$ and $K\alpha_1$ x rays, respectively, and $n(K\alpha_2)$ and $n(K\alpha_1)$ are the numbers of $K\alpha_2$ and $K\alpha_1$ x-ray photons in coincidence with which the $L$ x-ray spectra were measured.

$W(\theta)$ is a factor which corrects for the existing angular correlation[18] between the directions of emission of $K\alpha_1$ and $L\alpha$ x rays (while relative to the direction of emission of $K\alpha_2$ x rays, the $L\alpha$ x rays are emitted isotropically), and is given by the expression $W(\theta)=1+Q_2A_2P_2(\cos\theta)$, where $\theta$ is the angle between the direction of propagation of the radiations incident on the $K$ and $L$ x-ray detectors, $P_2(\cos\theta)$ is the second-order Legendre polynomial, $A_2$ is the angular correlation coefficient for the $K\alpha_1$-$L\alpha$ cascade, and $Q_2$ is a geometrical correction factor dependent on the energies of the $K\alpha_1$ and $L\alpha$ x rays and on the solid angles subtended by the detectors at the x-ray source. $W(\theta)$ can be made to equal 1 by choosing $\theta=125.26°$ in which case $P_2(\cos\theta)=0$.

The accuracy of the values of $f_{23}$ obtainable by this method is highly dependent on the extent to which the experiment can resolve the various x-ray transitions involved in the measurement and in particular correct the data for contributions of $L$ x rays in coincidence with $K\alpha_1$ x rays to the measured spectrum of $L$ x rays in coincidence with $K\alpha_2$ x rays.

The advent in the mid 1960s of high-resolution solid-state silicon and germanium x-ray spectrometers facilitated the task considerably and enabled measurements of $f_{23}$ with greatly improved accuracy, especially in the higher-$Z$ atoms where the energy separation between the various x-ray transitions is also larger. Methods have also been developed for cases where quite extensive overlap exists between the $K\alpha_1$ and $K\alpha_2$ x-ray spectra.[17,19]

Unfortuantely, however, even in the most favorable cases and with the best available spectrometers the intrusion of $K\alpha_1$ x rays into the $K\alpha_2$ region of the measured x-ray spectrum cannot be avoided and its precise determination has therefore continued to present a challenge and be a limiting factor to the accuracy of the results obtainable.

A case in point is the determination of the value of $f_{23}$ in Pb($Z=82$).

The two latest reported values for $f_{23}$ in Pb are $0.130\pm0.002$ by Tan *et al.*[20] and $0.112\pm0.002$ by Campbell *et al.*[21] In both these works the authors used state-of-the-art experimental techniques including high-energy-resolution silicon and germanium detectors and multiparameter coincidence systems with data recording in the list mode which offered full monitoring of all experimental parameters.

The two works differ however in the method used for calculating the previously mentioned important correction of the data for the intrusion of $K\alpha_1$ x rays into the $K\alpha_2$ region of the spectrum. Campbell *et al.*[21] calculated the extent of this intrusion by decomposing the measured $K$ x-ray spectrum into three components, $K\alpha_1$, $K\alpha_2$, and $K\alpha_3$, using for each component a standard shape defined by analytical functions with parameters

 

obtained by a nonlinear least-squares best-fit technique. Tan *et al.*[20] determined $f_{23}$ from their data using two methods of analysis and in each method the contribution of $K\alpha_1$ x rays to the $K\alpha_2$ region of the spectrum was calculated differently. In one method this contribution was calculated by estimating the shape of the $K\alpha_1$ x-ray spectrum from the shapes of spectra of monoenergetic $\gamma$ rays of like energy. In the second method the shape of the $K\alpha_1$ x-ray spectrum was estimated from the shape of the $K\alpha_2$ x-ray spectrum; this latter spectrum was separated from the other components of the $K$ x-ray spectrum by coincidence measurements with $L\gamma$ x rays.

However, the values of $f_{23}$ obtained in these two works differ from one another by more than the range of their estimated experimental errors and also happen to lie on opposite sides of the latest theoretically calculated value of 0.122 (Ref. 22) thus giving no indication as to the direction in which theoretical improvement is to be sought.

The present author has previously reported a value of $f_{23}$ in Pb of $0.1055\pm0.0011$.[23] This value was obtained using an experimental system very similar to the systems used in the above-mentioned works[20,21] but employing a different method of data analysis.

It is the purpose of the present paper to provide a definitive account of the work performed and its final result and describe in some detail the method used in the data analysis.

## II. EXPERIMENTAL SETUP

### A. X-ray source and detectors

The Pb x rays were obtained from a source of radioactive 38-year $^{207}$Bi which decays to $^{207}$Pb by electron capture,[24] predominatly by $K$-electron capture, initiating $K$-$L$ x-ray cascades in the Pb atom.

A source of $^{207}$Bi 2 mm in diameter and of approximately 30 $\mu$Ci intensity was used. It was prepared by drying a droplet of $^{207}$Bi in $HNO_3$ solution on a 1-mil-thick Mylar film.

The $K$ x rays were detected with a liquid-nitrogen-cooled hyperpure germanium detector, Ge(HP), 10 mm in diameter and 5 mm thick with an energy resolution of 480 eV at 122 keV. The $L$ x rays were detected with a liquid-nitrogen-cooled lithium-drifted silicon detector, Si(Li), 4 mm in diameter and 3 mm thick with an energy resolution of 180 eV at 5.9 keV. The relative angle between the detectors was 135° or 225°, randomly changed between experimental runs.

### B. Electronic system

A schematic diagram of the electronic system is shown in Fig. 1.

The pulses from the Si(Li) crystal were passed through a low-noise cryogenic preamplifier into an amplifier with several outputs, each of which was optimized for either timing or pulse height (energy) resolution. A fast bipolar output from the amplifier, optimized for timing resolution, was taken to a timing single-channel analyzer set to pass the entire pulse-height spectrum above the electronic noise level while a second output, optimized for energy resolution, went into an 8192-channel analog-to-digital converter (ADC). The single-channel analyzers had two outputs, one providing the starting pulses for a time-to-amplitude converter (TAC) and the second taken to a scaler to be counted for general monitoring purposes.

The pulses from the germanium detector were routed similarly except that the timing output from the single-

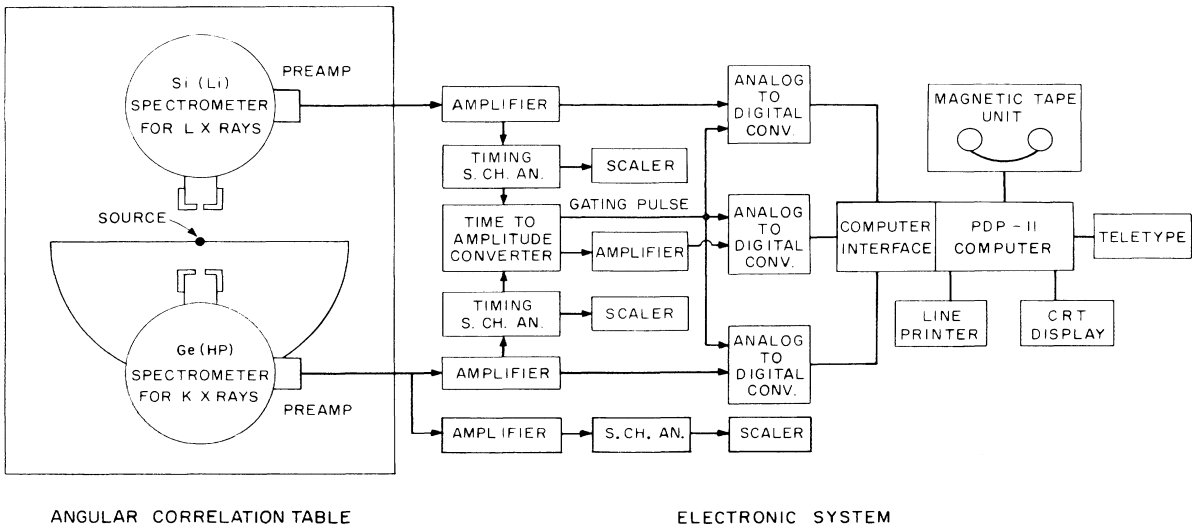


FIG. 1. Schematic diagram of experimental setup.

channel analyzer went to the stop, rather than the start, input of the time-to-amplitude converter through a variable-delay box used for time calibration of the time-to-amplitude converter. The timing single-channel analyzers had provisions for delaying their output pulses over the range of 0 to 11 $\mu$sec.

For the pulses from the preamplfier of the germanium detector a second route was established as well. It included an amplifier, single-channel analyzer set to pass only the $K$ x-ray region of the spectrum, and a scaler, and was used as yet another means of monitoring the stability of the system.

The time-to-amplitude converter was set for a range of 3 $\mu$sec and its output went through an amplifier to a 8192-channel analog-to-digital converter.

A logic output pulse from the time-to-amplitude converter indicating the reception of a stop input pulse within 3 $\mu$sec of a start input pulse was taken as an indicator of a valid coincidence event and used to derive a gating pulse to trigger the operation of the three analog-to-digital converters and the computer interface.

## III. DATA ACQUISITION AND ANALYSIS

### A. Acquisition and sorting of basic experimental data

Data acquistion was performed in the "list mode", i.e, for each coincidence event the computer recorded three parameters, the output values from the three analog-to-digital converters which are proportional respectively to the energies of the coincident $K$ and $L$ x rays and to the time interval between their detection. This last parameter allowed the separation of true coincidences from random ones. During the measurements the computer recorded on magnetic tape a list of such triads which could subsequently be sorted to build histograms showing the spectrum of one parameter for arbitrarily set conditions (digital gates) on the other two. For preset gates the computer was capable of sorting the data during the acquisition process itself and recording the resulting histograms in memory simultaneously with the recording of the full list data on tape.

The experiment consisted of 19 runs performed during a period of one month and ranging in duration from 19 to 125 hours. In ten of the runs data were acquired in full list mode on tape while histograms were recorded in memory, in six of the runs only histograms in memory were acquired, and in three runs full list mode data and histograms were acquired while the Si(Li) detector was shielded with aluminum absorbers of various thicknesses. The purpose of these last three runs was to check for possible contributions to the data from interdetector scattering, as will be explained in detail in Sec. IV.

The data acquired in each experimental run were sorted to yield the following nine spectra $S_1$ to $S_9$.

(a) $S_1$ and $S_2$. Spectra of $L$ x rays in coincidence with $K\alpha_2$ and $K\alpha_1$ x rays, respectively. In sorting the data to obtain these two spectra the $K\alpha_1$ and $K\alpha_2$ x rays were defined by setting digital gates on the output of the analog-to-digital converter which processed the pulses from the germanium detector corresponding to energy windows 680 eV wide, centered on the photopeaks resulting from the detection of the corresponding x rays. (See Fig. 2, windows $G_2$ and $G_1$, respectively.) The condition of coincidence was defined by setting a digital gate on the output of the analog-to-digital converter which processed the pulses from the time-to-amplitude converter corresponding to a time window 250 nsec wide centered on the prompt coincidence peak in the spectrum of pulses from the analog-to-digital converter (see Fig. 4).

(b) $S_3$. Spectrum of $L$ x rays in coincidence with radiation which deposited in the germanium detector an amount of energy within a window 680 eV wide (i.e., of equal width to the windows set on the $K\alpha_1$ and $K\alpha_2$ photopeaks) centered at an energy $E_{BK}$ which is below the energy $E_{K\alpha_2}$ of the $K\alpha_2$ photopeak by the same amount that $E_{K\alpha_2}$ is below $E_{K\alpha_1}$, the energy of the $K\alpha_1$ photopeak (see Fig. 2, window $G_3$).

This spectrum, as will be seen in detail in Sec. III D is crucial in determining the contribution of $L$ x rays coincident with $K\alpha_1$ x rays to the measured spectrum of $L$ x rays in coincidence with $K\alpha_2$ x rays.

(c) $S_4$. Spectrum of $L$ x rays in coincidence with radiation which deposited in the germanium detector an amount of energy within a window set above the energy of the $K\alpha_1$ photopeak (see Fig. 2, window $G_4$). This spectrum was used to determine the contribution of coincidences with higher-energy radiations to the three previous spectra.

(d) $S_5$. Spectrum of $L$ x rays in coincidence with $K\beta$ x rays. The $K\beta$ x rays were defined by the energy window $G_5$ shown in Fig. 2. $K\beta$ x rays and $L$ x rays are not emitted in coincidence in the same atomic cascade. They can occur in coincidence only if two x-ray cascades follow one another within a time interval shorter than the resolving time of the coincidence system. Such would be the case when in the course of nuclear deexcitation two processes resulting in inner-shell vacancies occur in quick succession, e.g., $K$-shell electron capture followed by internal conversion in the $K$ or $L$ shell in a subsequent nuclear transition. Such coincidences which

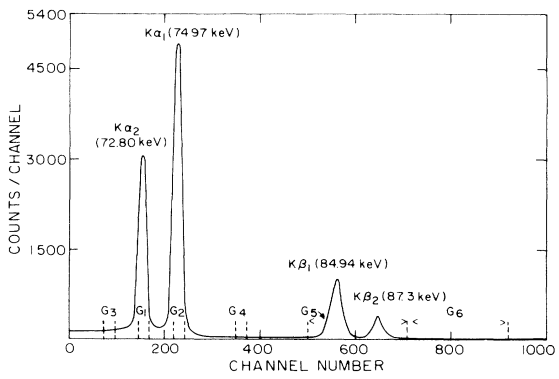


FIG. 2. Spectrum of $K$ x rays of Pb from electron-capture decay of $^{207}$Bi measured with cooled Ge(HP) spectrometer in random coincidence with L x rays. $G_1$ to $G_6$ mark the locations of the windows or digital gates set on the various parts of the spectrum as explained in Sec. III A.

have been called in the literature "nuclear"[25] or "nonrelated"[26] coincidences can involve of course not only $K\beta$ x rays but $K\alpha_1$ and $K\alpha_2$ x rays as well and will therefore contribute to the spectra $S_1$ to $S_3$. These contributions will be subtracted by making use of the spectrum $S_5$ and the intensity ratios $I(K\alpha_1)/I(K\beta)$, $I(K\alpha_2)/I(K\beta)$, etc.[25,26]

(e) $S_6$. Spectrum of $L$ x rays in coincidence with radiation which deposited in the germanium detector an amount of energy within a window set above the $K\beta$ photopeaks (see Fig. 2, window $G_6$). This spectrum was used to determine the contribution of coincidences with higher-energy radiations to spectrum $S_5$.

(f) $S_7$. Spectrum of $L$ x rays in *random coincidence* with radiation which deposited in the germanium detector an amount of energy within a window of 68–98 keV which included all $K$ x-ray peaks of interest in the present work (Fig. 3). The condition of random coincidence was defined by setting digital gates on the output of the analog-to-digital converter which processed the pulses from the time-to-amplitude converter corresponding to two time windows 1000 nsec wide each, on the two sides of the prompt coincidence peak and well separated from it (see Fig. 4). This spectrum was used, with proper normalization, to determine the contribution of random coincidences to all previously mentioned $L$ x-ray spectra.

(g) $S_8$. Spectrum of $K$ x rays in *random coincidence* with radiation which deposited in the silicon detector an amount of energy within a window of 8–17 keV, i.e., the energy range of the previously mentioned $L$ x-ray spectra $S_1$ to $S_7$. It should be noted that this spectrum and the previous one are derived from the analysis of the same (random) coincidence events, each spectrum showing the distribution of a different parameter. They also provide good representations of the spectra of radiation detected by the two detectors without any coincidence requirements.

(h) $S_9$. Spectrum of output pulses from the time-to-amplitude converter. This spectrum (see Fig. 4) was obtained for monitoring purposes only.

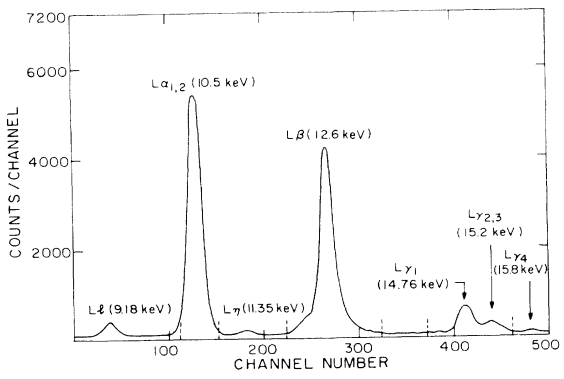


FIG. 3. Spectrum of $L$ x rays of Pb from electron-capture decay of $^{207}$Bi measured with cooled Si(Li) spectrometer in random coincidence with $K$ x rays. The dashed lines mark the portions of the spectrum assigned in the data analysis to the $L\alpha$, $L\beta$, and $L\gamma$ peaks.

### B. Processing of the raw x-ray spectra

The $L$ x-ray spectra enumerated in the previous section underwent the following stages of processing in succession.

(1) Removal of random coincidences. From each of the spectra $S_1$ to $S_6$ the contribution of random coincidences was removed by subtraction of spectrum $S_7$ multiplied by a normalization constant. For each spectrum $S_i$ ($i=1,6$) the constant is the product of (a) the ratio of the time intervals within the range of the time-to-amplitude converter (250 nsec/2000 nsec) allocated to the collection of true (spectra $S_1$ to $S_6$) and random (spectrum $S_7$) coincidences and (b) the ratio of the number of counts in spectrum $S_8$ within the window $G_i$ (see Fig. 2) used to acquire spectrum $S_i$ to the total number of counts in spectrum $S_8$.

(2) Removal from spectra $S_1$, $S_2$, $S_3$, and $S_5$ of contributions due to coincidences with higher-energy radiations. This correction was accomplished by subtracting spectrum $S_4$ from spectra $S_1$ to $S_3$ and spectrum $S_6$ from spectrum $S_5$ on the assumption that higher-energy radiation contributes a background which can be approximated by a constant number of counts per channel in the small energy intervals involved. All spectra involved were previously corrected for random coincidences in stage (1).

(3) Removal of contributions due to "nuclear" coincidences from spectra $S_1$, $S_2$, and $S_3$. This correction, the nature of which was explained in the previous section was accomplished by subtraction of spectrum $S_5$ multiplied by a normalization constant from spectra $S_1$

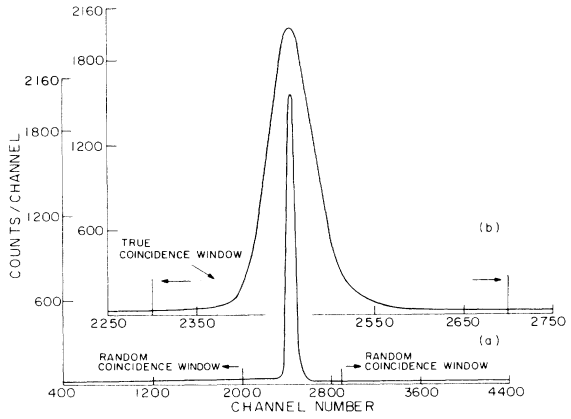


FIG. 4. Spectrum of output pulses from the time-to-amplitude converter. Each channel represents 0.625 nsec. (a) The true coincidence peak is shown on a flat background due to random coincidence events. The upper boundary of the lower 1-$\mu$sec window and the lower boundary of the upper 1-$\mu$sec window used to define random coincidence events are marked. (b) Enlarged portion of the spectrum showing the true coincidence peak and the 250-nsec window used to define true coincidence events.

to $S_3$. The normalization constant for spectrum $S_i$ ($i=1-3$) is the ratio of the (net) number of counts in spectrum $S_8$ within the window $G_i$ used to acquire spectrum $S_i$ to the (net) number of counts within window $G_5$. The net number of counts within each window was determined by subtracting from the raw number of counts within the window contributions due to higher-energy radiations assumed to amount to a constant number of counts per channel equal to the average number of counts per channel in the energy regions just above the peaks. Prior to this correction the spectra $S_1$ to $S_3$ and $S_5$ underwent corrections in stages (1) and (2).

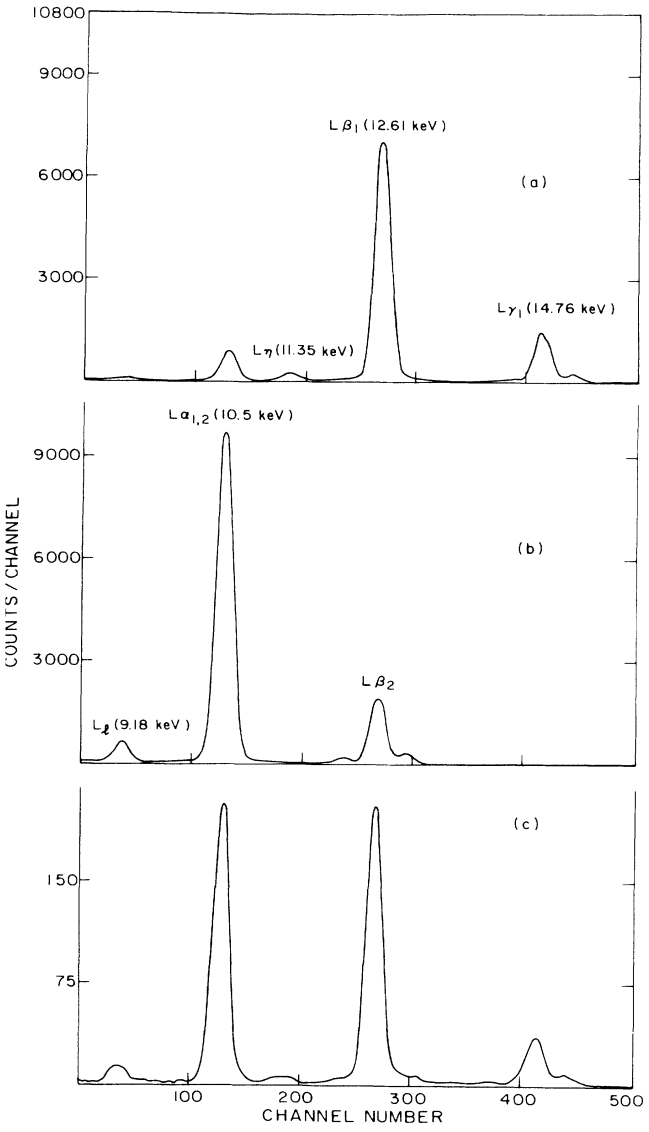


FIG. 5. (a) $S_{Lx}(K\alpha_2)$, (b) $S_{Lx}(K\alpha_1)$, and (c) $S_{Lx}$(BK) are spectra of $L$ x rays in coincidence with radiation, which deposited in the germanium detector energy within windows set on the $K\alpha_2$ and $K\alpha_1$ photopeaks and below the $K$ x-ray peaks (BK), respectively. The spectra are shown following the implementation of all the corrections described in Sec. III B.

### C. Resulting spectra and nomenclature

The three $L$ x-ray spectra resulting from $S_1$, $S_2$, and $S_3$ after the implementation of the previously described corrections will be denoted by $S_{Lx}(K\alpha_2)$, $S_{Lx}(K\alpha_1)$, and $S_{Lx}$(BK) to indicate $L$ x-ray spectra in coincidence with radiation which deposited in the germanium detector energy within windows set on the $K\alpha_2$ and $K\alpha_1$ photopeaks and below the $K$ x-ray peaks (BK). These spectra are shown in Fig. 5. The number of counts in a given peak $Lx$ in one of these spectra will be denoted by $N_{Lx}$(BK), $N_{Lx}(K\alpha_2)$, or $N_{Lx}(K\alpha_1)$, e.g., $N_{L\alpha}(K\alpha_1)$ denotes the number of counts in the $L\alpha$ x-ray peak in spectrum $S_{Lx}(K\alpha_1)$.

In obtaining these numbers the $L$ x-ray peaks were defined by the energy windows shown in Fig. 3 and from each peak, contributions due to higher-energy radiations were subtracted assuming a constant number of background counts per channel equal to the average number of counts per channel in the energy region just above the peak.

The number of counts within the windows $G_1$, $G_2$, and $G_3$ in spectrum $S_8$, corrected for contributions from higher-energy radiations will be denoted by $N(K\alpha_2)$, $N(K\alpha_1)$, and $N$(BK), respectively. Contributions to $N_{Lx}$(BK) or $N_{Lx}(K\alpha_i)$ and $N$(BK) due to radiation $K\alpha_j$ will be denoted by $N_{Lx}^{K\alpha_j}$(BK) or $N_{Lx}^{K\alpha_j}(K\alpha_i)$ and $N^{K\alpha_j}(K\alpha_i)$, respectively.

### D. Calculation of the contribution of $K\alpha_1$ x rays to the $K\alpha_2$ photopeak [and consequently of coincidences wth the $K\alpha_1$ x rays to the coincidence spectrum $S_{Lx}(K\alpha_2)$]. The fraction $R$

In order to calculate $f_{23}$ using expression (1) we need the quantities $C_{L\alpha}(K\alpha_1)$, $C_{L\alpha}(K\alpha_2)$, and $n(K\alpha_1)$ and $n(K\alpha_2)$. Assuming no contribution of the lower-energy $K\alpha_2$ x rays to the $K\alpha_1$ photopeak we may set $C_{L\alpha}(K\alpha_1)$ and $n(K\alpha_1)$ equal to $N_{L\alpha}(K\alpha_1)$ and $N(K\alpha_1)$, respectively, which are calculated as explained in the previous section.

The quantities $N_{L\alpha}(K\alpha_2)$ and $N(K\alpha_2)$ do, however, contain contributions due to the higher-energy $K\alpha_1$ x rays. Using the nomenclature adopted in the previous section we may write

$$C_{L\alpha}(K\alpha_2)=N_{L\alpha}(K\alpha_2)-N_{L\alpha}^{K\alpha_1}(K\alpha_2)\ , \tag{2}$$

$$n(K\alpha_2)=N(K\alpha_2)-N^{K\alpha_1}(K\alpha_2)\ . \tag{3}$$

Similarly,

$$N_{Lx}(\mathrm{BK})=N_{Lx}^{K\alpha_1}(\mathrm{BK})+N_{Lx}^{K\alpha_2}(\mathrm{BK})\ . \tag{4}$$

$$N(\mathrm{BK})=N^{K\alpha_1}(\mathrm{BK})+N^{K\alpha_2}(\mathrm{BK})\ . \tag{5}$$

It is assumed that no other than $K\alpha_1$ and $K\alpha_2$ radiations contribute to the coincident spectra or to windows $G_3$ and $G_1$. Small contributions due to other than $K\alpha_1$ and $K\alpha_2$ radiations, e.g., $K\alpha_3$ x rays, will be corrected for in the final result.

We will now define a quantity $R$ which is the ratio between the number of counts contributed by $K\alpha_1$ x rays

to the window $G_1$ set on the $K\alpha_2$ photopeak and the number of counts within the window $G_2$ set on the $K\alpha_1$ photopeak itself. Thus,

$$R=\frac{N^{K\alpha_1}(K\alpha_2)}{n(K\alpha_1)}=\frac{N^{K\alpha_1}(K\alpha_2)}{N(K\alpha_1)} . \tag{6}$$

We will now assume that $K\alpha_2$ x rays contribute to the window $G_3$ a fraction of their contribution to the $K\alpha_2$ photopeak itself equal to $R$ above, since the window $G_3$ is separated from the $K\alpha_2$ photopeak by the same energy interval that the window $G_1$ is separated from the $K\alpha_1$ photopeak. This is the same assumption used by Gnade *et al.*[16,19] and also implicit in the work of Tan *et al.*[20] when the shape of the $K\alpha_1$ spectrum is modeled by a shifted $K\alpha_2$ spectrum. Thus,

$$N^{K\alpha_2}(\mathrm{BK})=Rn(K\alpha_2) . \tag{7}$$

The contribution of coincidences with $K\alpha_1$ x rays to the spectrum $S_{Lx}(K\alpha_2)$ can be subtracted by assuming that each count due to $K\alpha_1$ x rays within the window $G_1$ set on the $K\alpha_2$ peak contributes a fraction $1/N(K\alpha_1)$ of the spectrum $S_{Lx}(K\alpha_1)$. The resulting spectrum which will be denoted by $S_{Lx}^{K\alpha_2}(K\alpha_2)$ is therefore given by the expression

$$S_{Lx}^{K\alpha_2}(K\alpha_2)=S_{Lx}(K\alpha_2)-\frac{N^{K\alpha_1}(K\alpha_2)}{N(K\alpha_1)}S_{Lx}(K\alpha_1) , \tag{8}$$

which by (6) can be written as

$$S_{Lx}^{K\alpha_2}(K\alpha_2)=S_{Lx}(K\alpha_2)-RS_{Lx}(K\alpha_1) . \tag{9}$$

Similarly, spectrum $S_{Lx}(\mathrm{BK})$ can be expressed as a linear combination of spectra $S_{Lx}(K\alpha_1)$ and $S_{Lx}^{K\alpha_2}(K\alpha_2)$ by assuming that each count due to $K\alpha_2$ x rays within the window $G_3$ contributes a fraction $1/n(K\alpha_2)$ of spectrum $S_{Lx}^{K\alpha_2}(K\alpha_2)$, while each count due to $K\alpha_1$ x rays within the window contributes $S_{Lx}(K\alpha_1)/N(K\alpha_1)$. Thus

$$S_{Lx}(\mathrm{BK})=\frac{N^{K\alpha_2}(\mathrm{BK})}{n(K\alpha_2)}S_{Lx}^{K\alpha_2}(K\alpha_2)+\frac{N^{K\alpha_1}(\mathrm{BK})}{N(K\alpha_1)}S_{Lx}(K\alpha_1) . \tag{10}$$

Expressions (8), (9), and (10) and their preceding explanatory statements hold true for the spectra $S_{Lx}^{K\alpha_2}(K\alpha_2)$, $S_{Lx}(K\alpha_2)$, $S_{Lx}(K\alpha_1)$, and $S_{Lx}(BK)$, channel by channel. It should be noted here that the assumption used in writing expressions (8) and (10), which was also used by Campbell *et al.*[21] was shown by Gnade *et al.*[19] not to be always correct since the pulses contributing to the tail of a given peak may have a different time structure than those contributing to the peak itself and thus may not be registered as coincidences when the coincidence system is operated with an insufficiently large resolving time window. Campbell *et al.*[21] ensured coincidence registration of all events by selecting in their work only pulses with rise times within a given time range and by using a sufficiently large resolving time window in their coincidence system.

In the present work no selection of pulses according to rise time was made. However, a very large resolving time window was employed which, as can be seen in Fig. 4, ensures registration of all coincidence events. As a check, some of the data were also sorted using a resolving time only half as large, with almost identical results. Furthermore, as will be explained in Sec. IV the present method of data analysis contains an internal consistency check which will provide a warning in case the above assumption does not hold. Using (5) and (7) in expression (10) we obtain

$$S_{Lx}(\mathrm{BK})=RS_{Lx}^{K\alpha_2}(K\alpha_2)+\frac{[N(\mathrm{BK})-N^{K\alpha_2}(\mathrm{BK})]}{N(K\alpha_1)}S_{Lx}(K\alpha_1) . \tag{11}$$

Substituting for $S_{Lx}^{K\alpha_2}(K\alpha_2)$ from expression (9) into (11) we obtain

$$S_{Lx}(\mathrm{BK})=R[S_{Lx}(K\alpha_2)-RS_{Lx}(K\alpha_1)]+\frac{[N(\mathrm{BK})-N^{K\alpha_2}(\mathrm{BK})]}{N(K\alpha_1)}S_{Lx}(K\alpha_1) . \tag{12}$$

Substituting again from (7) $N^{K\alpha_2}(\mathrm{BK})=Rn(K\alpha_2)$ and for $n(K\alpha_2)$ from (3) and (6) $n(K\alpha_2)=N(K\alpha_2)-RN(K\alpha_1)$ we will obtain

$$S_{Lx}(\mathrm{BK})=RS_{Lx}(K\alpha_2)-R^2S_{Lx}(K\alpha_1)+\frac{[N(\mathrm{BK})-RN(K\alpha_2)+R^2N(K\alpha_1)]}{N(K\alpha_1)}\times S_{Lx}(K\alpha_1) \tag{13}$$

or

$$S_{Lx}(\mathrm{BK})=RS_{Lx}(K\alpha_2)+\frac{N(\mathrm{BK})}{N(K\alpha_1)}S_{Lx}(K\alpha_1)-\frac{RN(K\alpha_2)}{N(K\alpha_1)}S_{Lx}(K\alpha_1) . \tag{14}$$

Expression (14) holds true for the spectra $S_{Lx}(\mathrm{BK})$, $S_{Lx}(K\alpha_2)$, and $S_{Lx}(K\alpha_1)$ channel by channel and therefore also for sums of any number of channels. In the present work it will be applied to the sums of the channels which make up the $L\alpha$, $L\beta$, and $L\gamma$ peaks. We can thus write

$$N_{Lx}(\mathrm{BK})=RN_{Lx}(K\alpha_2)+\frac{N(\mathrm{BK})}{N(K\alpha_1)}N_{Lx}(K\alpha_1)-\frac{RN(K\alpha_2)}{N(K\alpha_1)}N_{Lx}(K\alpha_1) , \tag{15}$$

where the subscript $Lx$ in $N_{Lx}(\mathrm{BK})$ and $N_{Lx}(K\alpha_i)$ stands for the $L\alpha$, $L\beta$, or $L\gamma$ peak.

Solving Eq. (15) for $R$ we finally obtain

$$R=\frac{N_{Lx}(\mathrm{BK})N(K\alpha_1)-N(\mathrm{BK})N_{Lx}(K\alpha_1)}{N_{Lx}(K\alpha_2)N(K\alpha_1)-N(K\alpha_2)N_{Lx}(K\alpha_1)} . \tag{16}$$

All the quantities appearing in this expression can be calculated from the final corrected spectra.

It should be noted that expression (16) is particularly simple when $Lx$ stands for the $L\gamma$ peak. Since $N_{L\gamma}(K\alpha_1)=0, R$ reduces simply, as expected, to the fraction $N_{L\gamma}(\mathrm{BK})/N_{L\gamma}(K\alpha_2)$. Once $R$ is known all other quantities necessary for the determination of $f_{23}$ can be calculated.

Thus $C_{L\alpha}(K\alpha_2)$ can be calculated using expression (9) and summing for the channels in the $L\alpha$ peak. We will obtain

$$C_{L\alpha}(K\alpha_2)=N_{L\alpha}(K\alpha_2)-RN_{L\alpha}(K\alpha_1) . \quad (17)$$

$n(K\alpha_2)$ was already shown above to be equal to $N(K\alpha_2)-RN(K\alpha_1)$.

Substituting for $C_{L\alpha}(K\alpha_2)$ and $n(K\alpha_2)$ in (1) we will obtain

$$f_{23}=\frac{[N_{L\alpha}(K\alpha_2)-RN_{L\alpha}(K\alpha_1)]N(K\alpha_1)}{N_{L\alpha}(K\alpha_1)[N(K\alpha_2)-RN(K\alpha_1)]} \times[1+Q_2A_2P_2(\cos\theta)] , \quad (18)$$

which after rearrangement will yield:

$$f_{23}=\frac{\left[\frac{N_{L\alpha}(K\alpha_2)}{N_{L\alpha}(K\alpha_1)}-R\right]}{\left[\frac{N(K\alpha_2)}{N(K\alpha_1)}-R\right]}[1+Q_2A_2P_2(\cos\theta)] . \quad (19)$$

## IV. RESULTS AND DISCUSSION

For each experimental run, separate calculations of $R$ were made using Eq. (16) with data obtained from the $L\alpha$, $L\beta$, and $L\gamma$ peaks. The weighted average of these $R$ values was then used to calculate $f_{23}$ for the given run from Eq. (19) in which the angular correlation correction factor was taken as 1.009 based on a previous measurement.[27] The weighted average of the values of $f_{23}$ obtained in the 16 runs was then calculated and found to be $(11.02\pm0.09)\times10^{-2}$. This value has to be still slightly corrected upward for the minute contribution of $K\alpha_3$ x rays to the $K\alpha_2$ peak (0.164% according to calculations[28]) leading to a result for $f_{23}$ of $(11.04\pm0.09)\times10^{-2}$. The errors listed are statistical only, each being one standard deviation of the mean.

As a check on the internal consistency of the results, weighted averages were calculated of the values of $R$ obtained in the 16 runs using data from the $L\alpha$, $L\beta$, and $L\gamma$ peaks. They were found to be respectively, $(2.238\pm0.070)\times10^{-2}$, $(2.144\pm0.033)\times10^{-2}$, and $(2.480\pm0.045)\times10^{-2}$.

As can be seen, the values of $R$ obtained using data from the $L\alpha$ and $L\beta$ peaks agree within experimental errors, while the value of $R$ obtained using data from the $L\gamma$ peak is somewhat higher.

In an attempt to find the reason for this slight discrepancy it was noted that the value of $R$ calculated using data from the $L\gamma$ peak is, because of the relatively low intensity of the $L\gamma$ transition, very sensitive to even slight contributions of erroneous coincidences to the quantity $N_{L\gamma}(\mathrm{BK})$. Such contributions may occur as a result of Compton scattering of $K$ x-ray radiation in the Si(Li) detector and the detection of the scattered x ray in the germanium detector. In order to estimate the contributions of such scattering events to $N_{L\gamma}(\mathrm{BK})$, and to all coincidence spectra in general, three experimental runs were performed in which the Si(Li) detector was shielded from the direct radiation of the source by aluminum absorbers 71.4 mg/cm$^2$ thick in one run and 285.6 mg/cm$^2$ thick in the other two runs. These absorbers, while attenuating extensively and to various degrees the $L\alpha$, $L\beta$, and $L\gamma$ x rays, are almost transparent to the $K$ x rays and higher-energy radiations, thus emphasizing the contributions of coincidences due to scattering as compared to true $K$-$L$ x-ray coincidences. These experiments showed that there were no contributions of coincidences due to scattering to the $L\alpha$ or $L\beta$ peaks in any of the coincidence spectra while slight contributions to the $L\gamma$ peak were present and caused the value of $R$ calculated using $L\gamma$ peak data to increase. The poor statistics of the scattering experiments did not allow, however, a precise measurement of these scattering contributions and therefore a determination as to whether they accounted fully or only partially for the observed increase in the value of $R$ calculated using $L\gamma$ peak data.

It was also noted that the value of $R$ calculated using $L\alpha$ peak data is very sensitive to contributions to $N(\mathrm{BK})$ from other than $K\alpha_1$ and $K\alpha_2$ x rays. Therefore, the fact that the value of $R$ obtained using data from the $L\alpha$ peak is almost identical to that obtained using data from the $L\beta$ peak is indicative that no such foreign contributions to the $K$ x-ray spectrum in the region below the $K\alpha_2$ peak were present. Note that this also implies that the pulses contributing to the tail of the $K$ x-ray peaks are registered in the coincidence experiments with the same efficiency as those contributing to the peaks themselves (otherwise they would be considered in this case foreign contributions to the spectrum).

The value of $R$ calculated using data from the $L\beta$ peak was found to be least sensitive to both coincidences due to scattering as well as to foreign contributions to the $K$ x-ray spectrum in the region below the $K\alpha_2$ peak. This value of $R$ is therefore the most reliable. It also has the smallest statistical error. If in each experimental run only this value of $R$ is used in the calculation of $f_{23}$ rather than the weighted average of the three values of $R$ obtained from $L\alpha$, $L\beta$, and $L\gamma$ data the final result for $f_{23}$ is $(11.21\pm0.10)\times10^{-2}$ identical to the result obtained by Campbell *et al.*[21] This value will be taken as our final result.

## V. CONCLUSION

A method for the analysis of multiparameter $K$-$L$ x-ray coincidence data has been developed which is capable of yielding precise values for the Coster-Kronig transition probability $f_{23}$ in high $Z$ atoms. The method utilizes only ratios of quantities determined from the same coincidence measurement and is therefore relatively insensitive to small instabilities in the experimental

system. The method does not require any auxiliary measurements beyond the coincidence measurements and contains internal consistency checks which alert the user to possible systematic errors.

In the present work the use of this method to determine $f_{23}$ in Pb has been described. The result obtained, $0.112 \pm 0.001$ is identical to the result of Campbell *et al.*[21] and slightly lower than the latest theoretical value of 0.122.[6,22]

Preliminary values of $f_{23}$ obtained using this method in Tm and Pt have been reported[23,29] and a definitive account of the works is currently in preparation. The method is also currently being adapted for use in lower-$Z$ atoms.

Both the preliminary values of $f_{23}$ in Tm and Pt as well as values of $f_{23}$ measured[3] in Au and recently[30] in Xe are slightly lower than those predicted by the latest theoretical calculations,[6] thus seemingly confirming the trend pointed to by the value of $f_{23}$ in Pb.

## ACKNOWLEDGMENT

I wish to thank Mr. Richard Volpicelli for his assistance with the electronic system.

[1]W. Bambynek, B. Crasemann, R. W. Fink, H. U. Freund, H. Mark, C. D. Swift, R. E. Price, and P. Venugopala Rao, Rev. Mod. Phys. **44**, 716 (1972). This paper contains many references to previous works.

[2]L. Salgueiro, M. T. Ramos, M. L. Escrivao, M. C. Martins, and J. G. Ferreira, J. Phys. B **7**, 342 (1974).

[3]W. Jitschin, G. Materlik, U. Verner, and P. Funke, J. Phys. B **18**, 1139 (1985).

[4]E. J. McGuire, Phys. Rev. A **3**, 587 (1971); and in Proceedings of the International Conference on Inner Shell Ionization Phenomena and Future Applications, edited by R. W. Fink, S. T. Manson, J. M. Palms, and P. Venugopala Rao [U.S. Atomic Energy Commission Report No. CONF-720404, 1973 (unpublished)], Vol. I, p. 662.

[5]M. H. Chen, E. Laiman, B. Crasemann, M. Aoyagi, and H. Mark, Phys. Rev. A **19**, 2253 (1979).

[6]M. H. Chen, B. Crasemann, and H. Mark, Phys. Rev. A **24**, 177 (1981).

[7]J. C. McGeorge, D. W. Nix, and R. W. Fink, J. Phys. B **6**, 573 (1973).

[8]J. L. Campbell, L. A. McNelles, J. S. Geiger, R. L. Graham, and J. S. Merritt, Can. J. Phys. **52**, 488 (1974).

[9]V. R. Veluri, R. E. Wood, J. M. Palms, and P. Venugopala Rao, J. Phys. B **7**, 1486 (1974).

[10]M. R. Zalutsky and E. S. Macias, Phys. Rev. A **11**, 71 (1975).

[11]M. R. Zalutsky and E. S. Macias, Phys. Rev. A **11**, 1093 (1975).

[12]D. W. Nix and R. W. Fink, Z. Phys. A **273**, 305 (1975).

[13]D. W. Nix and R. W. Fink, Z. Phys. A **278**, 239 (1976).

[14]M. H. Chen, B. Crasemann, and V. O. Kostroun, Phys. Rev. A **4**, 1 (1971).

[15]M. H. Chen and B. Crasemann, in Proceedings of the International Conference on Inner Shell Ionization Phenomena and Future Applications, edited by R. W. Fink, S. T. Manson, J. M. Palms, and P. Venugaopala Rao [U.S. Atomic Energy Commission Report No. CONF-720404, 1973 (unpublished)], Vol. I. p. 43.

[16]P. Venugopala Rao, R. E. Wood, J. M. Palms, and R. W. Fink, Phys. Rev. **178**, 1997 (1969).

[17]B. E. Gnade, R. A. Braga, and R. W. Fink, Phys. Rev. C **21**, 2025 (1980); **23**, 580(E) (1981).

[18]A. L. Catz, Phys. Rev. A **2**, 634 (1970).

[19]B. E. Gnade, R. A. Braga, W. R. Western, J. L. Wood, and R. W. Fink, Nucl. Instrum. Methods **164**, 163 (1979).

[20]M. Tan, R. A. Braga, R. W. Fink, and P. V. Rao, Phys. Scr. **25**, 536 (1982).

[21]J. L. Campbell, P. L. McGhee, R. R. Gingerich, R. W. Ollerhead, and J. A. Maxwell, Phys. Rev. A **30**, 161 (1984).

[22]According to Ref. 20 this value was calculated by M. H. Chen using the method described in Ref. 6.

[23]A. L. Catz, Bull. Am. Phys. Soc. **23**, 116 (1978).

[24]C. M. Lederer, V. S. Shirley, E. Browne, J. M. Dairiki, R. E. Doebler, A. A. Shihab-Eldin, L. J. Jardine, J. K. Tuli, and A. B. Buyrn, *Table of Isotopes,* 7the ed. (Wiley, New York, 1978).

[25]J. C. McGeorge, H. U. Freund, and R. W. Fink, Nucl. Phys. A **154**, 526 (1970).

[26]A. L. Catz and E. S. Macias, Phys. Rev. A **9**, 87 (1974).

[27]A. L. Catz and H. N. Erten, Bull. Am. Phys. Soc. **18**, 635 (1973).

[28]J. H. Scofield, Phys. Rev. A **9**, 1041 (1974).

[29]A. L. Catz, Bull. Am. Phys. Soc. **23**, 622 (1978).

[30]P. B. Semmes, R. A. Braga, J. C. Griffin, and R. W. Fink, Phys. Rev. C **35**, 749 (1987).